

Chattering Free with Noise Reduction in Sliding-Mode Observers Using Frequency Domain Analysis

M. Hajatipour, M. Farrokhi*

Department of Electrical Engineering,
Iran University of Science and Technology, Tehran 16846, IRAN

This paper presents analysis and regulation of switching in the sliding-mode observers for nonlinear systems. First, the high gain property of the sliding observer is employed in order to obtain fast convergence of the estimated states to the system ones. Then, when the system is in the switching condition, signals are decomposed into two modes: the slow mode and the fast mode. The observer parameters are designed based on the relay feedback systems such that the high gain property is provided for the slow mode operation. This ensures fast convergence of the estimated states and at the same time, by controlling the fast mode of the observer, the high frequency oscillations (i.e. the chattering phenomena) can be rejected by a simple low-pass filter. In addition, the behavior of the proposed observer is analyzed in the presence of the measurement noise. Moreover, a variable relay-equivalent gain technique will be introduced to make the proposed observer less sensitive to measurement noises and to maintain good estimation of the states. The proposed nonlinear observer is tested through simulations in an illustrative example involving a bioreactor. Simulation results show good performance of the proposed method as compared to the conventional sliding-mode observer.

Keywords: Sliding-mode observers; Relay-feedback systems; High-gain observers; Nonlinear Systems; Switching frequency; Bioreactor

1. Introduction

Sliding-mode observers are known to be robust against presence of disturbances and modeling uncertainties [1–3]. Although these observers are highly robust with respect to noises in system inputs, it turned out that the corresponding stability degrades in systems that exhibit output noise or mixed uncertainties [4]. When the measurements are noisy, because the time derivatives cannot be accurately calculated, it can lead to poor closed-loop performance or instabilities in the estimation procedure.

Sliding-mode observers are known as high-gain observers, which have appropriate behavior in disturbance rejection [5–7]. Vasiljevic and Khalil have shown that a high-gain observer acts as a differentiator in the limit as the gain approaches infinity [8]. Hence, in the presence of the measurement noise, it magnifies the noise in the estimated states. Therefore, there is a trade-off between the observer gain and the noise effect in the state estimation. In addition, they have showed that a bound on the estimation error exists that depends on the maximum amplitude of the measurement noise. Recently, Ahrens and Khalil have introduced a high-gain observer, where the gain matrix switches between two values [9]. In this method, when the estimation error reaches a steady-state threshold, it switches to a second gain to reduce the effect of the measurement noise. The idea of gain switching in observers has been employed before by other researchers for noise cancellation in the state estimation [10].

Since the main source of the sliding phenomena is the relay element, researchers use relay feedback systems to analyze sliding properties [11]. Due to the interesting characteristics of relay feedback systems, research in this area is fast developing. A number of analyzing methods for the modeling of relay feedback systems as well

as methods for estimating the switching frequencies and the amplitude of oscillations are discussed in [12, 13]. It is well known that when the relay feedback system is operating in the switching mode, it may have finite or infinite switching frequencies, which are called the limit cycle and the ideal sliding mode, respectively.

For the first time, Boiko and Fridman applied the relay feedback concept to the design of linear observers, where they have used the relay equivalent gain technique [14, 15]. In continuation of their works, a novel approach for the observer design for nonlinear systems in presence of the measurement noise is presented in this paper. The proposed method takes advantage of the high-gain observers in order to enforce the estimated states to move quickly to the system states. Therefore, in the first step, the conditions for forcing the observer to go to the switching zone are satisfied. Next, when the observer is operating in the switching or the sliding condition, the signals are decomposed into two parts: the slow-mode part and the fast-mode part. For every mode, the corresponding design for the appropriate operation of the observer will be considered. It will be shown that the amplitude and frequency of oscillations have direct effects on the dynamics and stability of the fast and slow-modes of the states estimation when the observer is operating in the switching condition. Moreover, in order to make the proposed observer robust against the measurement noise, first the performance of the observer in presence of the measurement noise is analyzed. Next, the effect of the measurement noise in states estimation will be considerably reduced by introducing a Variable Relay-Equivalent Gain (VREG) technique. The main features of this paper can be summarized as follows:

- Frequency regulation of the sliding-mode observer without any need for linearization
- Presenting a relationship between the switching frequency and stability and the performance of sliding-mode observers
- Providing high gain property in the switching mode for sliding-mode observers and consequently obtaining fast convergence of the estimated states to the actual states
- Proposing a variable gain technique in order to have less sensitivity to the measurement noise in sliding-mode observers.

Simulation results show good performance of the proposed method as compared to the conventional sliding-mode observers in a bioreactor application.

This paper is organized as follows. Section 2 gives the problem statement, preliminary definitions, and assumptions. Section 3 provides the design procedure of the proposed method. Section 4 presents measurement noise analysis. Section 5 shows illustrative example followed by conclusions in Section 6.

Notations: Throughout this paper, $\lambda_{\max}(\mathbf{A})$ denotes the maximum eigenvalue of matrix \mathbf{A} and $\|\mathbf{A}\|$ denotes the 2-norm of it.

2. Problem statement

Consider the following class of systems:

$$\begin{aligned}\dot{\mathbf{x}} &= \mathbf{A}\mathbf{x} + \mathbf{f}(\mathbf{x}, u) + \mathbf{E}\lambda(\mathbf{x}, u) \\ y &= \mathbf{C}\mathbf{x}\end{aligned}\tag{1}$$

where $\mathbf{x} \in \mathfrak{R}^n$ is the vector of unknown state variables, $u \in \mathfrak{R}^m$ is the input signal, $y \in \mathfrak{R}$ is the measured output, $\mathbf{f} : \mathfrak{R}^n \times \mathfrak{R} \rightarrow \mathfrak{R}^n$ is a nonlinear smooth function, $\mathbf{E} \in \mathfrak{R}^{n \times 1}$ and $\lambda : \mathfrak{R}^n \times \mathfrak{R}^m \rightarrow \mathfrak{R}$ is the modeling uncertainties and disturbances, respectively.

Assumption 1: An estimation gain \mathbf{L} can be designed such that $(\mathbf{A}-\mathbf{LC})$ is stable.

Assumption 2: The uncertainty function λ is assumed to be bounded; that is, $\|\lambda(\mathbf{x},u)\| \leq \bar{\lambda}$, where $\bar{\lambda}$ is the upper bound.

Assumption 3: The nonlinear function $\mathbf{f}(\mathbf{x},u)$ is Lipschitz with respect to \mathbf{x} and uniformly for $u \in \mathfrak{U}$, where \mathfrak{U} is an admissible control set. That is, there exists a constant $\gamma > 0$ such that

$$\|\mathbf{f}(\mathbf{x},u) - \mathbf{f}(\hat{\mathbf{x}},u)\| \leq \gamma \|\mathbf{x} - \hat{\mathbf{x}}\| \quad (2)$$

The following observer is proposed for system (1):

$$\mathbf{G}_{OBS}(s) := \begin{cases} \dot{\hat{\mathbf{x}}} = \mathbf{A}\hat{\mathbf{x}} + \mathbf{f}(\hat{\mathbf{x}},u) + \mathbf{L}(y - \hat{y}) + \mathbf{E}\bar{u} \\ \hat{y} = \mathbf{C}\hat{\mathbf{x}} \end{cases} \quad (3)$$

where $\hat{\mathbf{x}}$ denotes the estimated state vector, \mathbf{L} is the observer matrix, and \bar{u} is a discontinuous signal with the following form:

$$\bar{u} = d \operatorname{sgn}(\sigma_y(t)), \quad (4)$$

in which $d \geq 0$ is the relay gain and

$$\sigma_y(t) = y(t) - \bar{y}(t) \quad (5)$$

$$\bar{Y}(j\Omega) = \hat{Y}(j\Omega)H(j\Omega), \quad (6)$$

where $\bar{Y}(j\Omega)$ and $\hat{Y}(j\Omega)$ are the Laplace transform of signals $\bar{y}(t)$ and $\hat{y}(t)$, respectively. Assume that $H(j\Omega)$ is designed such that in the frequency domain

$$H(j\Omega) \approx \begin{cases} 1 & \text{for } \Omega \leq \Omega_b \\ \Phi(j\Omega) & \text{for } \Omega > \Omega_b \end{cases} \quad (7)$$

where Ω_b is defined as the bandwidth frequency of the slow-mode of the observer in the switching mode, $\Phi(j\Omega)$ will be designed later on.

Defining the state estimation error as $\boldsymbol{\sigma} := \mathbf{x} - \hat{\mathbf{x}}$, the error dynamics becomes

$$\begin{aligned} \dot{\boldsymbol{\sigma}} &= \mathbf{A}\boldsymbol{\sigma} - \mathbf{L}(y - \hat{y}) + (\mathbf{f}(\mathbf{x},u) - \mathbf{f}(\hat{\mathbf{x}},u)) + \mathbf{E}\lambda(\mathbf{x},u) - \mathbf{E}\bar{u} \\ &= (\mathbf{A} - \mathbf{LC})\boldsymbol{\sigma} + (\mathbf{f}(\mathbf{x},u) - \mathbf{f}(\hat{\mathbf{x}},u)) + \mathbf{E}\lambda(\mathbf{x},u) - \mathbf{E}\bar{u} \end{aligned} \quad (8)$$

The proposed observer is designed for two different states: the transient state and the switching state. In the transient state, the observer is a high-gain observer. That is, the high gain of the relay (d) guarantees fast convergence of the estimation errors to zero and forcing the observer to enter the switching region. Moreover, the high gain can provide better disturbance rejection. It should be noted that, before the switching state (i.e. when the estimation error is large) the amplitude of the measurement noise is negligible as compared to the amplitude of the estimation error. Hence, the noise reduction does not play an important role when the estimation error is large. In the switching state, however, a novel approach will be proposed where the signals are decomposed into the slow and fast modes, each mode requiring a different design. In other words, the amplitude

and frequency of oscillations are defined such that the slow-mode of the observer in the switching mode behaves like a high gain observers. This provides very quick convergence of the slow-mode estimation error to zero. Moreover, by regulating the switching frequency, oscillations can simply be removed from the estimated states using a low-pass filter. In addition, a Variable Relay-Equivalent Gain (VREG) technique will be proposed to diminish noise effects on the estimated states. Hence, the objective is to design d , $H(s)$, and \mathbf{L} to achieve these goals.

Definition 1: Due to the presence of the discontinuity in the relay, signals in the switching mode can be decomposed into two parts: 1) the fast-mode part associated with the periodical motion across the switching surface and 2) the slow-mode part associated with the motion along the switching surface. Let define $\Omega \leq \Omega_b$ as the low frequency domain and $\Omega > \Omega_b$ as the high frequency domain. Therefore, every signal in the system and in the observer can be decomposed into two parts: 1) the slow-mode part and 2) the fast-mode part; i.e. $\mathbf{x} = \mathbf{x}_0 + \mathbf{x}_s$, $\sigma_y(t) = \sigma_{y_0}(t) + \sigma_{y_s}(t)$, $\boldsymbol{\sigma} = \boldsymbol{\sigma}_0 + \boldsymbol{\sigma}_s$, $y = y_0 + y_s$, $\hat{y} = \hat{y}_0 + \hat{y}_s$, $\bar{y} = \bar{y}_0 + \bar{y}_s$, where subscripts “0” and “s” indicate the slow and fast modes of the corresponding signal, respectively. This separating idea has been used before for linear systems by some researches such as [16] and [17].

Remark 1: As it will be considered later, since the frequency of the fast-mode can be designed high enough and far from the bandwidth of the slow-mode of the observer Ω_b , then by passing signals through a low-pass filter with a bandwidth greater than Ω_b but smaller than the switching frequency Ω_s , which is high enough, the high frequency mode can be removed from the estimated states. This idea was proposed before by other researchers such as [18]. Hence, the main system just observes the slow-mode of the estimated state variables, which has frequency in the domain of $\Omega \leq \Omega_b$. Without loss of generality, let assume that the main part of the system signals, which are going to be estimated, are in the frequency domain of $\Omega \leq \Omega_b$. In addition, the remaining part of the system signals, which is assumed to be in the domain of $\Omega > \Omega_b$ (e.g. measurement noises) is not important as compared to the high frequency mode of the observer and hence, can be ignored. Therefore, the high frequency parts of the main system signals, i.e. $y_s(t)$ and $\mathbf{x}_s(t)$, can be eliminated. In other words, it can be assumed that $\mathbf{x}_s = 0$ and $y_s(t) = 0$.

Proposition 1: Signal $\bar{y}(t)$ in the slow and fast-modes can be written as

$$\bar{y}(t) = \begin{cases} \hat{y}(t) & \text{for } \Omega \leq \Omega_b \\ \int_0^t \hat{y}(\tau) \varphi(t-\tau) d\tau & \text{for } \Omega > \Omega_b \end{cases} \quad (9)$$

respectively, where $\varphi(t)$ is the inverse Laplace transform of $\Phi(s)$ presented in (7). Moreover,

$$\sigma_{y_0}(t) = \mathbf{C} \boldsymbol{\sigma}_0(t) \quad (10)$$

$$\sigma_{y_s}(t) = -\mathbf{C} \left(\int_0^t \hat{\mathbf{x}}_s(t) \varphi(t-\tau) d\tau \right) \quad (11)$$

proof: Using (6) and (7), $\bar{y}(t)$ can be written as

$$\bar{y}(t) = \mathcal{L}^{-1} \left\{ \hat{Y}(j\Omega) H(j\Omega) \right\} \quad (12)$$

where $\mathcal{L}^{-1}\{\cdot\}$ indicates the inverse Laplace transform operator. The slow and fast modes of this signal are

$$\begin{aligned}\bar{y}_0(t) &= \mathcal{L}^{-1}\left\{\hat{Y}(j\Omega)H(j\Omega)\right\}\Big|_{\Omega \leq \Omega_b} \\ &= \mathcal{L}^{-1}\left\{\hat{Y}(j\Omega)\Big|_{\Omega \leq \Omega_b} H(j\Omega)\Big|_{\Omega \leq \Omega_b}\right\} \\ &= \int_0^t \hat{y}_0(\tau)\delta(t-\tau)d\tau = \hat{y}_0(t),\end{aligned}\tag{13}$$

$$\begin{aligned}\bar{y}_s(t) &= \mathcal{L}^{-1}\left\{\hat{Y}(j\Omega)H(j\Omega)\right\}\Big|_{\Omega > \Omega_b} \\ &= \mathcal{L}^{-1}\left\{\hat{Y}(j\Omega)\Big|_{\Omega > \Omega_b} H(j\Omega)\Big|_{\Omega > \Omega_b}\right\} \\ &= \int_0^t \hat{y}_s(\tau)\varphi(t-\tau)d\tau.\end{aligned}\tag{14}$$

Hence, the errors between the estimated and actual outputs in the slow and fast-modes are

$$\sigma_{y_0}(t) = y_0(t) - \bar{y}_0(t) = \mathbf{C}(\mathbf{x}_0(t) - \hat{\mathbf{x}}_0(t)) = \mathbf{C}\boldsymbol{\sigma}_0(t),\tag{15}$$

$$\begin{aligned}\sigma_{y_s}(t) &= y_s(t) - \bar{y}_s(t) = \mathbf{C}\mathbf{x}_s(t) - \left(\int_0^t \hat{y}_s(\tau)\varphi(t-\tau)d\tau\right) \\ &= \mathbf{C}\left(\mathbf{x}_s(t) - \left(\int_0^t \hat{\mathbf{x}}_s(\tau)\varphi(t-\tau)d\tau\right)\right).\end{aligned}\tag{16}$$

Then, according to Remark 1, using a low-pass filter, $\sigma_{y_s}(t)$ becomes

$$\sigma_{y_s}(t) = -\mathbf{C}\left(\int_0^t \hat{\mathbf{x}}_s(\tau)\varphi(t-\tau)d\tau\right).\tag{17}$$

The Laplace transform of (17) is

$$\Sigma_{y_s}(s) = -\mathbf{C}\hat{\mathbf{X}}_s(s)\Phi(s) = \mathbf{C}\Sigma_s(s)\Phi(s),\tag{18}$$

where $\Sigma_{y_s}(s) = \mathcal{L}\{\sigma_{y_s}(t)\}$, $\hat{\mathbf{X}}_s(s) = \mathcal{L}\{\hat{\mathbf{x}}_s(t)\}$ and $\Sigma_s(s) = \mathcal{L}\{\boldsymbol{\sigma}_s(t)\}$. \square

Remark 2: Decomposition of signals into the slow and fast modes is just needed in the switching state and in the normal operation (i.e. before the switching conditions occur) where signals operate in the frequency domain $\Omega \leq \Omega_b$. Hence, using (5) and Proposition 1, before the system enters into the switching state

$$\sigma_y(t) = \mathbf{C}\boldsymbol{\sigma}(t).\tag{19}$$

In the next section, the observer design for these two states (i.e. the transient state and the switching state) will be given.

3. Observer Design

In this section, the observer design will be presented for two different states. First, in the transient state, conditions for forcing the estimated state variables to move quickly to the switching state will be defined. Due to the high amplitude of the relay gain d , this mode acts as a high-gain observer. Next, in the switching state, parameters will be designed such that a fast transient is obtained for the slow-mode and a simple high-frequency rejection is provided for the fast-mode.

3.1. Transient state

In this subsection, it will be shown that proper selection of the relay parameter (d) guarantees convergence of the error dynamics to the sliding surface in finite time and that the switching condition occurs.

Let define $\sigma_y = 0$ as the sliding surface. It is well known that the sliding surface and its derivative must satisfy $\sigma_y = \dot{\sigma}_y = 0$ in the switching mode. The condition for existence of a switching mode is [19]:

$$\sigma_y \dot{\sigma}_y < 0 \quad \forall \sigma_y \neq 0 \text{ and } \forall t \geq t_0. \quad (20)$$

Then, it is said that the surface $\sigma_y = 0$ is an attracting surface and the switching condition occurs.

Assumption 4: Assume that the positive definite matrix $\mathbf{P}_1 = \mathbf{P}_1^T$ and matrix \mathbf{L} satisfy the following equation:

$$(\mathbf{A} - \mathbf{LC})^T \mathbf{P}_1 + \mathbf{P}_1^T (\mathbf{A} - \mathbf{LC}) = -\mathbf{Q}_1, \quad (21)$$

where \mathbf{A} is Hurwitz and \mathbf{Q}_1 is positive definite.

Assumption 5: Assume that $\boldsymbol{\sigma}^T \mathbf{N} \boldsymbol{\sigma} > 0$, where $\mathbf{N} = \mathbf{P}_1 \mathbf{E} \mathbf{C}$.

Lemma 1: Consider Assumptions 1--5, Remark 1, and the error dynamics (8) and (19). Selecting the sliding parameter d as

$$d \geq d_1 \quad (22)$$

where

$$d_1 = (-\lambda_{\min}(\mathbf{Q}_1) + \|\mathbf{P}_1\| \gamma) \|\boldsymbol{\sigma}(\mathbf{0})\| + \bar{\lambda} \|\mathbf{E}\| \|\mathbf{P}_1\| / \|\mathbf{E}\| \|\mathbf{P}_1\|$$

and $\boldsymbol{\sigma}(\mathbf{0})$ is $\boldsymbol{\sigma}(t)$ at $t = t_0$, guarantees that $\lim_{t \rightarrow \infty} \|\boldsymbol{\sigma}(t)\| = 0$. In addition, the sliding surface will reach the sliding manifold $\sigma_y = 0$ in finite time and the switching mode will occur.

Proof: Let define the following Lyapunov function:

$$V_1 = \frac{1}{2} \boldsymbol{\sigma}^T \mathbf{P}_1 \boldsymbol{\sigma}. \quad (23)$$

The time derivative of this function is

$$\begin{aligned} \dot{V}_1 &= \boldsymbol{\sigma}^T \mathbf{Q}_1 \boldsymbol{\sigma} + \boldsymbol{\sigma}^T \mathbf{P}_1 (f(\mathbf{x}, u) - f(\hat{\mathbf{x}}, u) - \mathbf{E} \lambda(\mathbf{x}, u)) - \boldsymbol{\sigma}^T \mathbf{P}_1 \mathbf{E} \bar{u} \\ &\leq -\lambda_{\min}(\mathbf{Q}_1) \|\boldsymbol{\sigma}\|^2 + \|\mathbf{P}_1\| \gamma \|\boldsymbol{\sigma}\|^2 + \bar{\lambda} \|\mathbf{E}\| \|\mathbf{P}_1\| \|\boldsymbol{\sigma}\| - d \boldsymbol{\sigma}^T \mathbf{P}_1 \mathbf{E} \frac{\mathbf{C} \boldsymbol{\sigma}}{\|\mathbf{C} \boldsymbol{\sigma}\|}. \end{aligned} \quad (24)$$

Considering Assumption 5 and the fact that $\mathbf{C} \boldsymbol{\sigma}$ is a scalar, it gives

$$\dot{V}_1 \leq (-\lambda_{\min}(\mathbf{Q}_1) + \|\mathbf{P}_1\| \gamma) \|\boldsymbol{\sigma}\|^2 + \bar{\lambda} \|\mathbf{E}\| \|\mathbf{P}_1\| \|\boldsymbol{\sigma}\| - d \mathbf{C} \frac{\boldsymbol{\sigma} \boldsymbol{\sigma}^T \mathbf{P}_1 \mathbf{E}}{\|\mathbf{C}\| \|\boldsymbol{\sigma}\|}, \quad (25)$$

Hence, \dot{V}_1 becomes negative if

$$d \mathbf{C} \frac{\boldsymbol{\sigma} \boldsymbol{\sigma}^T \mathbf{P}_1 \mathbf{E}}{\|\mathbf{C}\|} \geq (-\lambda_{\min}(\mathbf{Q}_1) + \|\mathbf{P}_1\| \gamma) \|\boldsymbol{\sigma}\|^3 + \bar{\lambda} \|\mathbf{E}\| \|\mathbf{P}_1\| \|\boldsymbol{\sigma}\|^2, \quad (26)$$

or equivalently

$$\begin{aligned}
d &\geq \frac{\left((-\lambda_{\min}(\mathbf{Q}_1) + \|\mathbf{P}_1\|\gamma)\|\boldsymbol{\sigma}\|^3 + \bar{\lambda}\|\mathbf{E}\|\|\mathbf{P}_1\|\|\boldsymbol{\sigma}\|^2 \right)\|\mathbf{C}\|}{\|\mathbf{C}\boldsymbol{\sigma}\boldsymbol{\sigma}^T\mathbf{P}_1\mathbf{E}\|} \\
&\geq \frac{\left((-\lambda_{\min}(\mathbf{Q}_1) + \|\mathbf{P}_1\|\gamma)\|\boldsymbol{\sigma}\|^3 + \bar{\lambda}\|\mathbf{E}\|\|\mathbf{P}_1\|\|\boldsymbol{\sigma}\|^2 \right)\|\mathbf{C}\|}{\|\mathbf{C}\|\|\boldsymbol{\sigma}\boldsymbol{\sigma}^T\|\|\mathbf{E}\|\|\mathbf{P}_1\|} \\
&\geq \frac{\left(-\lambda_{\min}(\mathbf{Q}_1) + \|\mathbf{P}_1\|\gamma \right)\|\boldsymbol{\sigma}\| + \bar{\lambda}\|\mathbf{E}\|\|\mathbf{P}_1\|}{\|\mathbf{E}\|\|\mathbf{P}_1\|}.
\end{aligned} \tag{27}$$

Now, let define

$$d_1 = \left(-\lambda_{\min}(\mathbf{Q}_1) + \|\mathbf{P}_1\|\gamma \right)\|\boldsymbol{\sigma}(\mathbf{0})\| + \bar{\lambda}\|\mathbf{E}\|\|\mathbf{P}_1\|/\|\mathbf{E}\|\|\mathbf{P}_1\|.$$

Hence, selecting $d \geq d_1$ guarantees $\dot{V}_1 < 0$. Consequently, $\|\boldsymbol{\sigma}(t)\| = 0$ can be reached in finite time.

Next, to show that the switching condition occurs, let define $V_2 = \frac{1}{2}\sigma_y^2$. According to (19), the time derivative of V_2 is

$$\begin{aligned}
\dot{V}_2 &= \sigma_y \dot{\sigma}_y \\
&= \sigma_y \mathbf{C} \left[\left((\mathbf{A} - \mathbf{L}\mathbf{C})\boldsymbol{\sigma} + \mathbf{f}(\mathbf{x}, u) - \mathbf{f}(\hat{\mathbf{x}}, u) + \mathbf{E}\lambda(\mathbf{x}, u) \right) - \mathbf{E}\bar{u} \right] \\
&\leq \|\sigma_y\| \left[\|\mathbf{C}\|\|\boldsymbol{\sigma}\| (\|\mathbf{A} - \mathbf{L}\mathbf{C}\| + \gamma) + \|\mathbf{C}\|\|\mathbf{E}\|\bar{\lambda} \right] - \mathbf{C}\mathbf{E}d \|\sigma_y\| \\
&= \|\sigma_y\| \left[\|\mathbf{C}\|\|\boldsymbol{\sigma}\| (\|\mathbf{A} - \mathbf{L}\mathbf{C}\| + \gamma) + \|\mathbf{C}\|\|\mathbf{E}\|\bar{\lambda} - \mathbf{C}\mathbf{E}d \right]
\end{aligned} \tag{28}$$

Since it was shown that $\|\boldsymbol{\sigma}\| \rightarrow 0$ and $d \geq d_1$, it can be readily seen that the last bracket of (28) becomes negative and consequently $\dot{V}_2 \leq 0$. Therefore, condition (22) ensures that the sliding surface $\sigma_y = 0$ can be reached in finite time and the switching condition occurs. \square

3.2. Switching state

It is well known that the describing function (DF) of relay elements in the switching state can be obtained based on its input amplitude and its d parameter [20]. Next, the DF for the relay element will be defined.

3.2.1 Relay model in the switching state

The relay element was defined in (4), where d is the relay gain and σ_y is the input defined in (5). As it will be shown latter, the fast-mode dynamics of the observer is a linear system. The oscillating and high frequency part of $\sigma_y(t)$ can be presented as [20]

$$\sigma_{ys}(t) = a \sin(\Omega_s t), \tag{29}$$

where a and Ω_s are the amplitude and frequency of the limit cycle (or oscillations), respectively. Using the Fourier transform, $\bar{u}(t)$ can be presented as [20]

$$\bar{u}(t) = K_n \sigma_{y0}(t) + K_s a \sin(\Omega_s t) + K_{s1} a \sin(2\Omega_s t) + \dots, \tag{30}$$

where K_n, K_s, K_{s1}, \dots can be determined using the Fourier transform. Hence, $\bar{u}(t)$ can be written as

$$\bar{u}(t) = K_n \sigma_{y0}(t) + K_s \sigma_{ys}(t) + N_\varepsilon(\cdot), \tag{31}$$

where $N_\varepsilon(\cdot)$ is the modeling error. Since Ω_s is selected high enough in the design procedure and because most systems in engineering applications act as low pass filters and in view of the fact that $N_\varepsilon(\cdot)$ contains signals with frequencies larger than Ω_s , the effect of $N_\varepsilon(\cdot)$ in the estimated states can be ignored without any loss of generality. Nevertheless, it will be considered in analysis.

Assumption 6: $N_\varepsilon(\cdot)$ is unknown but bounded and its norm can be presented as

$$\|N_\varepsilon(\cdot)\| < \beta_1 \|\sigma_0\| + \beta_2 \sigma_m, \quad (32)$$

where β_1 and β_2 are positive constants and $\sigma_m \geq a \geq \|\sigma_{ys}\|$.

Using (10), (31) can be written as

$$\bar{u}(t) = K_n \mathbf{C} \sigma_0(t) + K_s \sigma_{ys}(t) + N_\varepsilon(\cdot), \quad (33)$$

where K_n and K_s can be computed as [11, 20]

$$K_n = \left. \frac{\partial \bar{u}_0}{\partial \sigma_y} \right|_{\bar{u}_0=0} = \frac{2d}{\pi a}, \quad (34)$$

$$K_s = \frac{4d}{\pi a}. \quad (35)$$

Hence, the relay element passes the slow-mode of signals with the gain K_n and the fast-mode of signals with the gain K_s ; i.e.

$$\bar{u}_s(t) = K_s \sigma_{ys}(t), \quad (36)$$

$$\bar{u}_0(t) = K_n \mathbf{C} \sigma_0(t). \quad (37)$$

3.2.2 Observer structure in switching state

In order to derive the main results, first by considering two modes of signals in the switching state, let rewrite (8) as

$$\dot{\hat{\sigma}}_s + \hat{\sigma}_0 = \bar{\mathbf{A}} \hat{\sigma}_s + \bar{\mathbf{A}} \hat{\sigma}_0 + \mathbf{f}(\mathbf{x}_0 + \mathbf{x}_s, u) - \mathbf{f}(\hat{\mathbf{x}}_0 + \hat{\mathbf{x}}_s, u) + \lambda(\mathbf{x}_0 + \mathbf{x}_s, u) - \mathbf{E} \bar{u}, \quad (38)$$

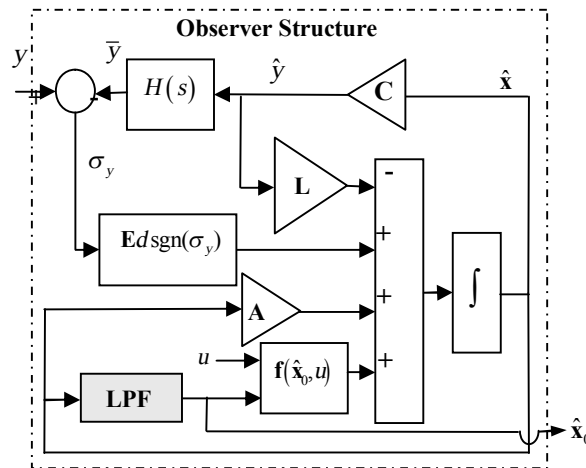


Figure 1. Block diagram of proposed observer.

where $\bar{\mathbf{A}} = \mathbf{A} - \mathbf{L}\mathbf{C}$. Note that based on Remark 1, the main system signals with high frequency modes (i.e. \mathbf{x}_s) can be eliminated from (38). Next, in the observer structure, the high frequency mode of estimated signals ($\hat{\mathbf{x}}_s$) is filtered if it is just used as states of a nonlinear function such as $\mathbf{f}(\cdot)$. This task changes the high frequency mode of the proposed observer into a linear system and consequently properties of the high frequency mode of the observer (such as the frequency and the relay equivalent gain), will obey linear relay feedback systems. Figure 1 presents the block diagram of the proposed observer, in which **LPF** denotes a linear Low Pass Filter, designed based on Remark 1.

Hence, (38) can be written as

$$\dot{\boldsymbol{\sigma}}_s + \dot{\boldsymbol{\sigma}}_0 = \bar{\mathbf{A}}\boldsymbol{\sigma}_s + \bar{\mathbf{A}}\boldsymbol{\sigma}_0 + \mathbf{f}(\mathbf{x}_0, u) - \mathbf{f}(\hat{\mathbf{x}}_0, u) + \mathbf{E}\lambda(\mathbf{x}_0, u) - \mathbf{E}\bar{u}. \quad (39)$$

Then, using (33)

$$\dot{\boldsymbol{\sigma}}_s + \dot{\boldsymbol{\sigma}}_0 = \bar{\mathbf{A}}\boldsymbol{\sigma}_s + \bar{\mathbf{A}}\boldsymbol{\sigma}_0 + \mathbf{f}(\mathbf{x}_0, u) - \mathbf{f}(\hat{\mathbf{x}}_0, u) + \mathbf{E}\lambda(\mathbf{x}_0, u) - K_n \mathbf{E}\mathbf{C}\boldsymbol{\sigma}_0(t) - K_s \mathbf{E}\boldsymbol{\sigma}_{ys}(t) - N_\varepsilon(\cdot)\mathbf{E}. \quad (40)$$

Consequently, the estimation error dynamics of the observer can be decomposed into the fast and slow modes, respectively, as

$$\mathbf{G}_{FO} : \dot{\boldsymbol{\sigma}}_s = (\mathbf{A} - \mathbf{L}\mathbf{C})\boldsymbol{\sigma}_s - K_s \mathbf{E}\boldsymbol{\sigma}_{ys}(t), \quad (41)$$

$$\mathbf{G}_{SO} : \dot{\boldsymbol{\sigma}}_0 = (\mathbf{A} - K_n \mathbf{E}\mathbf{C} - \mathbf{L}\mathbf{C})\boldsymbol{\sigma}_0 + \mathbf{f}(\mathbf{x}_0, u) - \mathbf{f}(\hat{\mathbf{x}}_0, u) + \mathbf{E}\lambda(\mathbf{x}_0, u) - N_\varepsilon(\cdot)\mathbf{E}, \quad (42)$$

where $\dot{\boldsymbol{\sigma}}_s$ and $\dot{\boldsymbol{\sigma}}_0$ are the observer error dynamics associated with the slow and fast modes, respectively. These two dynamics need to be designed for different modes. For the slow mode, K_n must be defined such that $\boldsymbol{\sigma}_0$ becomes very small as $t \rightarrow \infty$. On the other hand, in the fast-mode, $\mathbf{H}(j\Omega)$ and \mathbf{L} must be designed to provide proper values for K_n and in addition, the oscillation frequency becomes large enough. Moreover, to determine the relay equivalent gains K_n and K_s (as it will be shown in Theorem 3) there is a tradeoff between better state estimation and less sensitivity to the measurement noise.

3.2.2.1. Slow-mode dynamics of observer in switching state

Lemma 1 guarantees convergence of the error dynamics to the sliding surface, which in turn ensures occurrence of the switching state. Then, in the switching state, as it was shown in (41) and (42), the observer structure consists of two parts. In this section, K_n is designed such that the slow-mode of the estimation error, i.e. $\boldsymbol{\sigma}_0$, has small amplitude.

Assumption 7: Let $\mathbf{P}_2 = \mathbf{P}_2^T$ be a positive-definite matrix and also \mathbf{L} , \mathbf{E} and K_n be such that

$$(\mathbf{A} - \mathbf{E}\mathbf{C}K_n - \mathbf{L}\mathbf{C})^T \mathbf{P}_2 + \mathbf{P}_2^T (\mathbf{A} - \mathbf{E}\mathbf{C}K_n - \mathbf{L}\mathbf{C}) = -\mathbf{Q}_2 \quad (43)$$

where \mathbf{A} is the same as before and \mathbf{Q}_2 is a positive-definite matrix.

Theorem 1: Consider the slow-mode of the observation error (42) and Assumptions 1--7. Then, the error dynamics for the slow mode ($\boldsymbol{\sigma}_0$) is uniformly ultimately bounded. Moreover, this bound can be made small enough.

Proof: Consider the following Lyapunov function:

$$V_3 = \frac{1}{2} \boldsymbol{\sigma}_0^T \mathbf{P}_1 \boldsymbol{\sigma}_0 \quad (44)$$

where \mathbf{P}_1 is the same as defined in Assumption 4. The time derivative of (44) is

$$\begin{aligned} \dot{V}_3 &= -\boldsymbol{\sigma}_0^T \mathbf{Q}_1 \boldsymbol{\sigma}_0 + (\boldsymbol{\sigma}_0^T \mathbf{P}_1) (\mathbf{f}(\mathbf{x}_0, u) - \mathbf{f}(\hat{\mathbf{x}}_0, u) + \mathbf{E}\lambda(\mathbf{x}_0, u)) - K_n \boldsymbol{\sigma}_0^T \mathbf{P}_1 \mathbf{E} \mathbf{C} \boldsymbol{\sigma}_0 - N_\varepsilon(\cdot) (\boldsymbol{\sigma}_0^T \mathbf{P}_1 \mathbf{E}) \\ &\leq -\lambda_{\min}(\mathbf{Q}_1) \|\boldsymbol{\sigma}_0\|^2 + \gamma \|\mathbf{P}_1\| \|\boldsymbol{\sigma}_0\|^2 + \bar{\lambda} \|\mathbf{P}_1 \mathbf{E}\| \|\boldsymbol{\sigma}_0\| - K_n \lambda_{\min}(\mathbf{N}) \|\boldsymbol{\sigma}_0\|^2 + \|N_\varepsilon(\cdot)\| \|\boldsymbol{\sigma}_0\| \|\mathbf{P}_1 \mathbf{E}\|, \end{aligned} \quad (45)$$

where matrix \mathbf{N} was defined in Assumption 5. Using Assumption 6 and Young's inequality

$$\begin{aligned} \|\boldsymbol{\sigma}_0\| [\|N_\varepsilon(\cdot)\| \|\mathbf{P}_1 \mathbf{E}\| + \bar{\lambda} \|\mathbf{P}_1 \mathbf{E}\|] &\leq \|\boldsymbol{\sigma}_0\| \lambda_{\max}(\mathbf{P}_1) [\beta_1 \|\boldsymbol{\sigma}_0\| \|\mathbf{E}\| + \beta_2 \sigma_m \|\mathbf{E}\| + \bar{\lambda} \|\mathbf{E}\|] \\ &\leq \beta_1 \|\mathbf{E}\| \|\boldsymbol{\sigma}_0\|^2 \lambda_{\max}(\mathbf{P}_1) + \|\boldsymbol{\sigma}_0\| [\beta_2 \|\mathbf{E}\| \sigma_m \lambda_{\max}(\mathbf{P}_1) + \bar{\lambda} \|\mathbf{E}\|] \\ &\leq \|\boldsymbol{\sigma}_0\|^2 \left(\frac{1}{2} + \beta_1 \|\mathbf{E}\| \lambda_{\max}(\mathbf{P}_1) \right) + \frac{1}{2} [\beta_2 \|\mathbf{E}\| \sigma_m \lambda_{\max}(\mathbf{P}_1) + \bar{\lambda} \|\mathbf{E}\|]^2. \end{aligned} \quad (46)$$

Using (46), (45) becomes

$$\dot{V}_3 \leq -c_1 \|\boldsymbol{\sigma}_0\|^2 + c_2 \quad (47)$$

where $c_1 = \lambda_{\min}(\mathbf{Q}_1) + K_n \lambda_{\min}(\mathbf{N}) - \gamma \|\mathbf{P}_1\| - \beta_1 \|\mathbf{E}\| \lambda_{\max}(\mathbf{P}_1) - \frac{1}{2}$ and $c_2 = \frac{1}{2} [\beta_2 \|\mathbf{E}\| \sigma_m \lambda_{\max}(\mathbf{P}_1) + \bar{\lambda} \|\mathbf{E}\|]^2$.

Therefore, if K_n designed such that the following inequality holds:

$$\lambda_{\min}(\mathbf{Q}_1) + K_n \lambda_{\min}(\mathbf{N}) \geq \gamma \|\mathbf{P}_1\| + \beta_1 \|\mathbf{E}\| \lambda_{\max}(\mathbf{P}_1) + \frac{1}{2}, \quad (48)$$

and defining the following compact set around the origin:

$$\Psi := \left\{ \boldsymbol{\sigma}_0 \mid c_1 \|\boldsymbol{\sigma}_0\|^2 \leq c_2 \right\}, \quad (49)$$

it can be concluded that $\dot{V}_3 \leq 0$ when the error is outside of the compact set Ψ . Hence, according to the extension of the standard Lyapunov theorem [21], the error trajectory $\boldsymbol{\sigma}_0$ is ultimately bounded. Moreover, this bound can be made small using large values for c_1 . This can be accomplished by designing appropriate values for the observer parameters such as K_n and \mathbf{L} . \square

Remark 3: According to (49), by enlarging the equivalent relay gain K_n and consequently c_1 , the compact set Ψ becomes small. I.e., if K_n becomes large enough, then the radius of the compact set becomes negligible or $\|\boldsymbol{\sigma}_0\| \rightarrow 0$.

As it is clear from Theorem 1, in addition to vector \mathbf{L} , K_n also affects the dynamics of the slow-mode in the switching condition. In the next sections, it will be shown that K_n is a function of the amplitude and frequency of oscillations. Hence, K_n can be controlled by parameters of the fast-mode dynamics of the observer.

3.2.2.2. Fast-mode dynamics of observer in switching state

In Theorem 1, it was shown that the slow-mode of the observation error dynamics can become very small by the appropriate design of matrix \mathbf{L} and especially the gain of the slow mode (K_n). In the followings, the fast-mode of the observer in switching conditions is analyzed.

From (41) it can be shown that

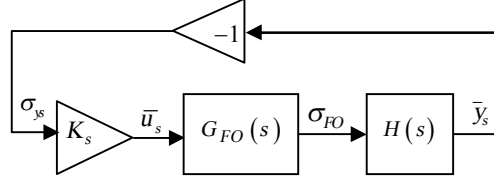


Figure 2. Fast-mode dynamics of observer

$$G_{FO} \equiv \begin{cases} \dot{\sigma}_s = (\mathbf{A} - \mathbf{L}\mathbf{C})\sigma_s + \mathbf{E}(-\bar{u}_s) \\ \sigma_{FO} = \mathbf{C}\sigma_s \end{cases} \quad (50)$$

where σ_{FO} is the output of the fast-mode dynamics of the observer and $-\bar{u}_s$, as shown in (36), is the input to the fast-mode observer as well as the output of the relay element. Hence, G_{FO} can be represented as

$$G_{FO}(s) = \frac{\mathcal{L}\{\mathbf{C}\sigma_s(t)\}}{\mathcal{L}\{-\bar{u}_s(t)\}} = -\frac{\mathbf{C}\Sigma_s(s)}{\bar{U}_s(s)}, \quad (51)$$

where $\bar{U}_s(s) = \mathcal{L}\{\bar{u}_s(t)\}$ and $\Sigma_s(s) = \mathcal{L}\{\sigma_s(t)\}$.

The next proposition demonstrates the relationship between the input and output signals of the relay element in the fast-mode in the frequency domain.

Proposition 2: Consider (18), (36) and (50). The relationship between the input and output of the relay element in the fast-mode is

$$\frac{\mathcal{L}\{\sigma_{ys}(t)\}}{\mathcal{L}\{\bar{u}_s(t)\}} = \frac{\Sigma_{ys}(s)}{\bar{U}_s(s)} = -G_{FO}(s)H(s) \quad (52)$$

where \bar{u}_s and σ_{ys} are the input and output of the relay element in the fast-mode operation, respectively.

Proof: From (36) we have $\bar{U}_s(s) = K_s \mathcal{L}\{\sigma_{ys}(t)\}$. Considering (18) and (51), it gives

$$\Sigma_{ys}(s) = \mathbf{C}\Sigma_s(s)\Phi(s) = -\bar{U}_s(s)G_{FO}(s)\Phi(s). \quad (53)$$

Hence, considering (7)

$$\frac{\Sigma_{ys}(s)}{\bar{U}_s(s)} = -G_{FO}(s)H(s), \quad (54)$$

where $\Sigma_{ys}(s)/\bar{U}_s(s)$ is equal to the inverse of the transfer function of the relay element in the fast-mode operation, i.e. $1/K_s$. Therefore,

$$\frac{1}{|K_s|} = |G_{FO}(j\Omega_s)||H(j\Omega_s)|. \quad (55)$$

This completes the proof. □

Figure 2 presents the fast-mode dynamics of the observer. On the other hand, using (34), (35) and (55), it gives

$$|K_n| = \frac{1}{2|G_{FO}(j\Omega_s)||H(j\Omega_s)|} \quad (56)$$

As it was shown in this section, the relay equivalent gain in the fast and slow modes can be regulated by the appropriate structure design of linear systems $G_{FO}(s)$ and $H(s)$ and also by the frequency of oscillations Ω_s . In other words, the larger $|G_{FO}(j\Omega_s)||H(j\Omega_s)|$, the smaller K_n and K_s . Based on Theorem 1, these parameters directly affect the stability and the estimation error of the observer.

Equations (34), (35), (55) and (56) help the designer to determine K_n , K_s and the frequency and amplitude of oscillations, which will be considered in the following section.

Parameters Design

According to Proposition 2 and from the theory of self-oscillating adaptive systems, based on relay feedback systems, $H(s)$ can be designed such that the frequency of the oscillations (or the limit cycle) Ω_s , with the following property [20]:

$$\angle G_{FO}(j\Omega_s) + \angle H(j\Omega_s) = -180^\circ, \quad (57)$$

can be controlled as desired. Moreover, the amplitude of oscillations in the fast-mode operation can be derived using (35) and (55) as

$$a = \frac{4d}{\pi} |G_{FO}(j\Omega_s)||H(j\Omega_s)|. \quad (58)$$

Since the amplitude of $|G_{FO}(j\Omega)|$ is a decreasing function with respect to the frequency, larger selections of Ω_s lead to smaller values for $|G_{FO}(j\Omega)|$ and larger values for K_n and K_s . Therefore, making the switching frequency large enough and far enough from the bandwidth of the slow-mode of the observer has two benefits: 1) The oscillating mode of signals can be easily removed using a low-pass filter and 2) According to Theorem 1 and (56), in the switching state, the relay equivalent gain becomes large. Hence, the observer acts as a high gain observers, which provides faster transient times and better disturbance rejections. This property moves the observer closer to the ideal sliding-mode condition, where the switching frequency grows to infinite. The following theorem shows conditions for the ideal sliding mode.

Theorem 2. If the transfer function $W_l(s)$ is a quotient of two polynomials $B_m(s)$ and $A_n(s)$ of degrees m and n , respectively, with non-negative coefficients, then for the existence of the ideal sliding mode, it is necessary that the relative degree $(n-m)$ of $W_l(s)$ be one or two.

Proof: See [16].

Remark 4: According to Theorem 2, when condition (57) is not satisfied (i.e. when the relative degree of $G_{FO}(s)H(s)$ is less than two, and for some systems with the relative degree equal to two), then the ideal sliding mode occurs.

In the ideally sliding-mode condition, the switching frequency grows with no bound. However, in practice, since the sampling time τ is not zero, the switching frequency cannot be infinite. In this condition, the oscillation frequency obeys the following equation [14, 16]:

$$\angle G_{FO}(j\Omega_s) + \angle H(j\Omega_s) + \angle \exp(-j\Omega_s \tau) = -180^\circ \quad (59)$$

Therefore, it can be concluded that for systems in which $G_{FO}(s)H(s)$ satisfies the ideal sliding-mode condition, the switching frequency grows to the largest possible switching frequency that it can be computed from (59).

Remark 5: According to the fast-mode dynamics of the observer G_{FO} , presented in (50), \mathbf{E} and \mathbf{L} should be such that conditions given in Theorem 2 (i.e. conditions for the ideal sliding mode) are satisfied.

As it will be shown in Theorem 3, the oscillation frequency or relay equivalent gains should not be very large to make the observer susceptible to measurement noises.

4. Noise Effect Reduction and Design of $H(s)$

In the last section, it was showed that $G_{FO}(s)$ can be determined by vectors \mathbf{E} and \mathbf{L} . In this section, the effects of the measurement noise on the estimated states are analyzed. Then, in order to suppress the measurement noise, a procedure for the design of $H(s)$, $G_{FO}(s)$ and d will be given.

4.1. Noise effect analysis

Assume the system output in (1) is corrupted with measurement noise as

$$y_\omega = \mathbf{C}\mathbf{x} + \omega, \quad (60)$$

where $y_\omega \in \mathfrak{R}$ indicates the noisy output signal of the system and $\omega \in \mathfrak{R}$ is an additive bounded noise with $|\omega| \leq \chi$.

Theorem 3: Consider the system in (1), the input signal of the relay in (10) and (11) and the noisy system output in (60). Then, increasing the amplitude of $|G_{FO}(j\Omega_s)||H(j\Omega_s)|$ decreases the noise effect in the fast and slow-modes of the input signal of the relay σ_{ys} , and hence, better estimation of states. Moreover, increasing the gain of the relay element d has the same effect on the fast-mode dynamics.

Proof: First, the noise effect on the fast-mode of σ_y is analyzed. Let y_ω be in the frequency domain of the fast-mode signals. Then, the fast-mode amplitude of (5) can be written in the frequency domain as

$$|\Sigma_{ys}(j\Omega_s)| = |Y_\omega(j\Omega_s) - \bar{Y}_s(j\Omega_s)| = a, \quad (61)$$

where a is the same as before (i.e. the amplitude of the input signal of the relay element), $Y_\omega(s) = \mathcal{L}\{y_\omega(t)\}$ and $\bar{Y}_s(s) = \mathcal{L}\{\bar{y}_s(t)\}$. Using (55), (5) can be written as

$$\bar{Y}_s(j\Omega_s) = Y_\omega(j\Omega_s) - K_s G_{FO}(j\Omega_s) H(j\Omega_s) \Sigma_{ys}(j\Omega_s). \quad (62)$$

Then, using (35) and (62), it gives

$$\left| \frac{\Sigma_{ys}(j\Omega_s)}{\bar{Y}_s(j\Omega_s)} \right| = \left| \frac{Y_\omega(j\Omega_s)}{\bar{Y}_s(j\Omega_s)} - 1 \right| = \left| \frac{|Y_\omega(j\Omega_s)|}{\sqrt{|Y_\omega(j\Omega_s)|^2 + \left| \frac{4d}{\pi} G_{FO}(j\Omega_s) H(j\Omega_s) \right|^2} - \frac{8d}{\pi} |G_{FO}(j\Omega_s) H(j\Omega_s) Y_\omega(j\Omega_s)|}} - 1 \right| \quad (63)$$

Clearly, by selecting d and $|G_{FO}(j\Omega_s)||H(j\Omega_s)|$ large enough, it results that $|\Sigma_{ys}(j\Omega_s)/\bar{Y}_s(j\Omega_s)| \approx 1$. This means that the effect of the noisy output signal to the relay input signal (i.e. σ_{ys}) will be reduced. Similarly, for the slow-mode domain, let assume y_ω be in the frequency domain of the slow-mode signals. Then, according to (37--42) and (60), G_{SO} in presence of measurement noise becomes

$$G_{SO} : \hat{\sigma}_0 = (\mathbf{A} - \mathbf{E}\mathbf{C}K_n - \mathbf{L}\mathbf{C})\sigma_0 + \mathbf{f}(\mathbf{x}_0, u) - \mathbf{f}(\hat{\mathbf{x}}_0, u) + \mathbf{E}\lambda(\mathbf{x}_0, u) - \mathbf{E}N_\varepsilon(\cdot) - K_n\mathbf{E}\omega \quad (64)$$

Hence, selecting K_n small enough decreases the influence of the measurement noise in the slow-mode of the observer.

As a consequence, larger values for $|G_{FO}(j\Omega_s)||H(j\Omega_s)|$ (or equivalently, smaller values for K_n) can suppress the effect of measurement noise in the state estimation. This can be achieved by the appropriate design of $|H(j\Omega_s)|$. \square

Remark 6: Since Theorem 3 and Lemma 1 provide two different values for the amplitude of the relay gain (d), the larger d should be selected, according to (63).

Remark 7: Based on Theorem 2, larger values for $|G_{FO}(j\Omega_s)||H(j\Omega_s)|$ are desired in order to reduce the effect of the measurement noise. However, according to (56) and Remark 3, this may yield longer transient times and less robustness to disturbance rejection due to small values of K_n . Therefore, the selection of the fast and slow-mode gains (K_s and K_n) is based on the tradeoff between the noise reduction and the robustness of the observer.

This fact suggests the design of a variable relay equivalent gain technique, where the gain should be large in order to obtain fast transient response and more robustness against disturbances. On the other hand, this gain should become smaller for better noise reduction. The procedure for designing this variable gain will be given in the following section.

4.2. Noise effect reduction using variable gain technique

This section provides a method that can help the sliding-mode observer to be less sensitive to the measurement noise. The design is based on the idea that adding a zero to the $G_{FO}(j\Omega_s)$ makes its amplitude larger in the switching mode, which in turn makes the amplitude of the gain K_n smaller (according to (56)). It is important to note that according to Theorem 2, adding a zero to the $H(s)$ brings the observer closer to the ideal sliding-mode conditions. In order to design a variable equivalent gain for the relay, consider the following structure for $H(j\Omega)$

$$H(j\Omega) = (1 + \alpha\gamma j\Omega), \quad (65)$$

where γ is a positive constant and $\alpha \geq 1$ is a variable parameter, which will be defined later on. The amplitude and the phase angle of $H(j\Omega)$ are

$$|H(j\Omega)| = \sqrt{1 + (\alpha\gamma\Omega)^2} \quad (66)$$

$$\angle H(j\Omega) = \tan^{-1}(\alpha\gamma\Omega). \quad (67)$$

According to (66), the amplitude of $H(j\Omega)$ varies proportionally with α . Therefore, according to (55) and (56), increasing α decreases K_n and K_s and vice versa.

As it was mentioned before and according to Remark 7, larger values of $|H(j\Omega_s)|$ makes the observer less sensitive to the measurement noise but incurs more state estimation errors, and vice versa. Hence, γ and α must be defined such that K_n is not too large and not too small.

Design of γ

On one hand, γ must be selected such that K_n is large enough to have fast response and better disturbance cancellation; this case corresponds to the minimum value of α (i.e. $\alpha_{\min} = 1$). On the other hand, γ must be selected such that K_n is small enough to have less sensitivity to the measurement noise, based on Theorem 3; this case corresponds to the maximum value of α .

Design of α

According to Theorem 1 and based on the inverse relationship between α and the relay equivalent gains in the fast and slow-modes (i.e. K_n and K_s), α must be equal to one to provide a high equivalent gain for the relay when the estimation error is significant. This will provide better performance for the state estimation and the disturbance rejection. Therefore, the minimum value of α is equal to one. On the other hand, when the estimation error is small enough, α must become larger to reduce the relay equivalent gain and consequently making the observer less sensitive to the measurement noise. It should be noted that α should not be very large since it makes K_n very small, which leads to slower tracking of the system states. Based on these points, a proper candidate for determining α is proposed as follows:

$$\alpha(\sigma_{y_0}) = 1 + \frac{0.5}{e^{(\frac{\lambda}{\chi})|\sigma_{y_0}|}}, \quad (68)$$

where χ is the upper bound of the norm of measurement noise. In (68), when the input signal of the relay element (σ_{y_0}) changes from χ to 0.2χ , α increases from 1.05 to 1.33, respectively. Consequently, K_n decreases from $K_0\sqrt{1+(\gamma\Omega)^2}/\sqrt{1+(1.05\gamma\Omega)^2}$ to $K_0\sqrt{1+(\gamma\Omega)^2}/\sqrt{1+(1.35\gamma\Omega)^2}$, respectively, where $K_0 = K_n$ for $\alpha = 1$. Figure 3 shows (68) for $\chi = 0.2$. The amplitude of K_n decreases when the estimation error (σ_{y_0}) is significant with respect to the measurement noise (i.e. when $\sigma_{y_0} \approx \chi$). Hence, when σ_{y_0} (i.e. the input signal to

relay element or the estimation error of system's output in the slow mode) becomes small, K_n and K_s decrease in order to have less sensitivity to the input measurement noise.

Based on the above discussions, the following criteria are proposed for the Variable Relay-Equivalent Gain (VREG) technique:

- γ is selected such that the amplitude of oscillations a (corresponding to $\alpha_{\min} = 1$) is approximately equal to $0.75\mathcal{X}$.
- α_{\max} is selected such that the amplitude of oscillations is approximately equal to $1.5\mathcal{X}$.

Remark 8: In (65), and based on the above procedure, γ is determined for $\Omega = \Omega_s$, where Ω_s is designed high enough and far from bandwidth of the system (Ω_b). Hence, γ will be a small constant, which in turn gives small values for $\alpha\gamma j\Omega$ in (69) for $\Omega < \Omega_b$. Hence, for $\Omega < \Omega_b$, we have $H(j\Omega) \approx 1$, which satisfies (7).

5. Application to Bioreactor

In this section, the performance of the proposed observer is illustrated using a typical bioreactor with biomass production and substrate concentration which belongs to the class of (1). The state equations of this bioreactor are [22, 23]

$$\begin{aligned}\dot{x}_1(t) &= \frac{\mu_m x_1(t) x_2(t)}{K_m x_1(t) + x_2(t)} - D x_1(t) \\ \dot{x}_2(t) &= -\frac{1}{Y} \frac{\mu_m x_1(t) x_2(t)}{K_m x_1(t) + x_2(t)} + (s_f - x_2(t)) D\end{aligned}\quad (69)$$

where the specific growth rate is assumed to follow the Contois model, x_1 is the biomass concentration, x_2 is the substrate concentration, s_f is the inlet substrate concentration, D is the dilution rate, K_m is the reaction constant, Y is the yield of cell mass, and μ_m is the maximal specific growth rate. It is assumed that the biomass $x_1(t)$ is measurable on line by a biosensor [24].

Farza et al. have shown that this system is observable [25]. In practice, μ_m and K_m may be uncertain and time-varying. Hence, let $\mu_m = \mu_m^0 + d_1(t)$ and $K_m = K_m^0 + d_2(t)$, where μ_m^0 and K_m^0 are the known nominal parameters, respectively, and $d_1(t)$ and $d_2(t)$ are model of the bounded additive time-varying parametric uncertainties, respectively. Hence, based on (1), the uncertain system is defined as

$$\begin{aligned}\dot{x}_1(t) &= \frac{\mu_m^0 x_1(t) x_2(t)}{K_m^0 x_1(t) + x_2(t)} - D x_1(t) + M(\mathbf{x}, t), \\ \dot{x}_2(t) &= -\frac{1}{Y} \frac{\mu_m^0 x_1(t) x_2(t)}{K_m^0 x_1(t) + x_2(t)} + (s_f - x_2(t)) D - \frac{1}{Y} M(\mathbf{x}, t)\end{aligned}$$

where $M(\mathbf{x}, t) = \frac{\mu_m x_1(t) x_2(t)}{K_m x_1(t) + x_2(t)} - \frac{\mu_m^0 x_1(t) x_2(t)}{K_m^0 x_1(t) + x_2(t)}$ is the unknown function.

The goal is to design a sliding mode observer based on (3) to estimate the process states in presence of the measurement noise and model uncertainties using the method developed in this paper.

In addition, the model and observer simulations have been carried out using a constant input substrate concentration and dilution rate. The parameter values used in simulations are as follows:

$$\mu_m^0 = 1\text{h}^{-1}, K_m^0 = 1, Y = 1, D = 0.5\text{h}^{-1}, s_f = 5 \text{ g.l}^{-1}, d_1 = 0.1\sin(1.5\pi t), d_2 = 0.05\sin(\pi t).$$

With these parameters, the uncertainty function $M(\mathbf{x}, t)$ is shown in Figure 4. The feedback gains (using the pole placement technique) are $\mathbf{L} = [2 \ -1]^T$, which satisfies conditions (21) and (48). Then, according to Lemma 1 and Theorem 3 the amplitude of the relay gain is $d = 50$.

The initial states of the system and the observer are selected as $\mathbf{x}(0) = [1 \ 1]^T$ and $\hat{\mathbf{x}}(0) = [0 \ 0.5]^T$, respectively. In order to show the fast switching property of the proposed method (Remark 5) \mathbf{E} and \mathbf{L} should be such that $G_{FO}(s)$ is stable and its relative degree is less than two. This provides the highest possible switching condition or the ideal sliding-mode condition. Since $\mathbf{E} = [1 \ -1]^T$ then it gives $G_{FO}(s) = 1/(s + 2.5)$, which has the relative degree of one with stable eigenvalue. Hence, the ideal sliding-mode occurs.

By selecting the sampling time equal to $\tau = 1 \times 10^{-4}$ s and considering (59), the switching frequency and the period of oscillations will be equal to $\Omega_s = 15700$ rad/s and $2\pi/\Omega_s = 4 \times 10^{-4}$ s, respectively. In this condition according to (56), the equivalent gain of the relay in the slow-mode of the proposed observer becomes

$$K_n = \frac{1}{2|G_{FO}(j\Omega_s)||H(j\Omega_s)|} = \frac{1}{2 \times (0.0006382) \times 1} = 7834.$$

Based on (58), the amplitude of oscillations is

$$a = \frac{4d}{\pi} |G_{FO}(j\Omega_s)||H(j\Omega_s)| = \frac{4 \times 50 \times 0.0006382}{\pi} = 0.0041.$$

Since the frequency of oscillations Ω_s is selected high enough, a simple low-pass filter can easily reject high frequency signals. The selected low-pass filter is

$$G(s) = 1/((0.0073s + 1)(0.0073s + 1)).$$

Figure 5 shows simulation results for σ_{ys} . As this Figure indicates, the period of oscillations and a are equal to 4×10^{-4} s and 45×10^{-4} , respectively, which confirms the values obtained from the equations.

Next, the effect of measurement noise on the state estimation is analyzed. The measurement noise is a white noise with uniform distribution in $[-0.2, 0.2]$. Hence, the bound of the measurement noise is equal to $\chi = 0.2$.

To improve the estimation accuracy in presence of the measurement noise, the proposed VREG technique, discussed in section 4.2, is applied here.

Figure 6 shows performance of the proposed method in noise reduction for state estimations for two cases: 1) Estimation using the conventional sliding mode observer with fixed relay equivalent gain, which is equal to $K_n = 7834$ (i.e. the same value that was used in the first part of simulations). This property is common with all conventional sliding-mode observers, where researchers use a relay element, 2) Sliding mode observer using the VREG technique with $\gamma = 2 \times 10^{-3}$ and $\alpha = 1 + (1/e^{10|\sigma_{y0}|})$.

As it was discussed before, in VREG technique, K_n is large when the estimation error is considerable and small when the estimation error is small. This property provides faster convergence of the estimation error and less sensitivity to the measurement noise as compared to the conventional sliding-mode observer.

Figure 7 shows the input signal of the relay element (σ_{ys}) using the conventional sliding-mode observer (i.e. with fixed gain) and the VREG technique in presence of the measurement noise. This figure shows that VREG technique provides less sensitivity to the measurement noise in the input signal of the relay element. That is, the oscillation frequency is fixed and is not affected by the noise. Figure 8 shows variations of α in VREG technique.

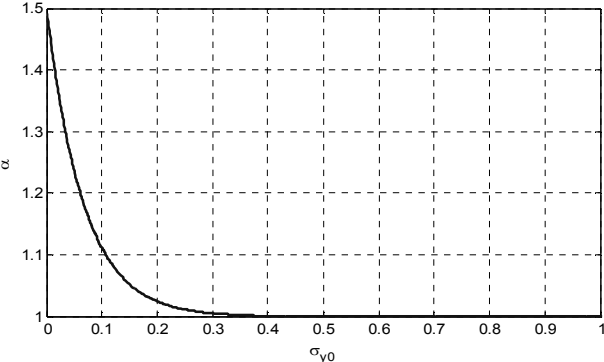


Figure 3. Variations of parameter α with respect to the input signal of the relay element σ_{y_0} when $\chi = 0.2$

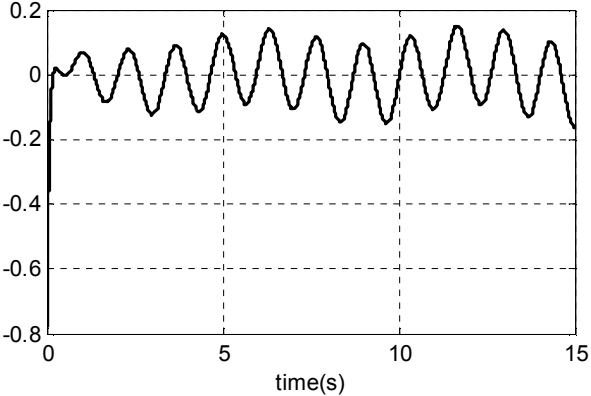


Figure 4. Signal $M(x,t)$

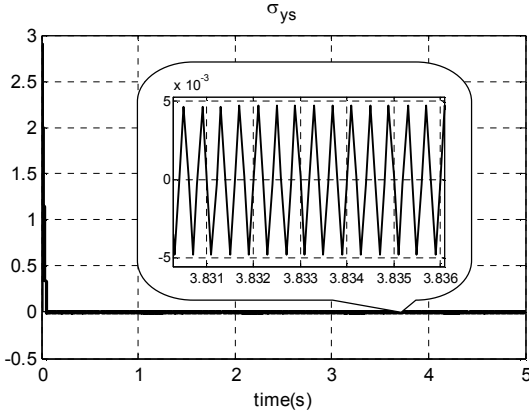
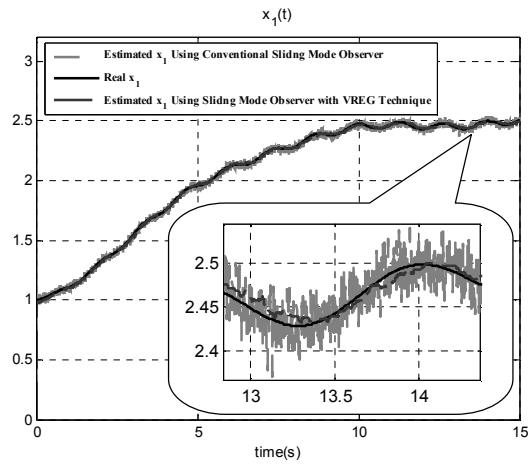
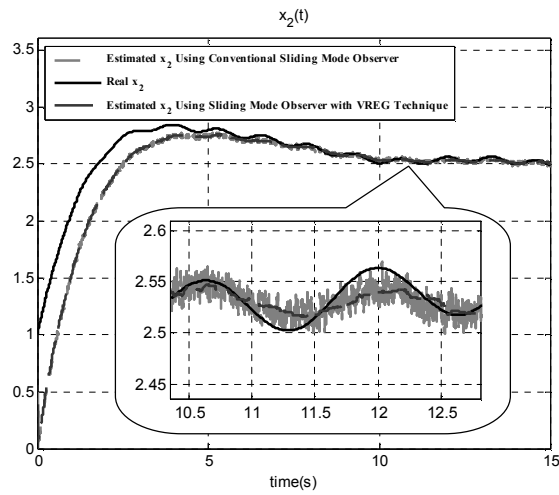


Figure 5. Signal σ_{ys} using conventional sliding mode observer



(a)



(b)

Figure 6. $x_1(t)$ and $x_2(t)$ in presence of measurement noise

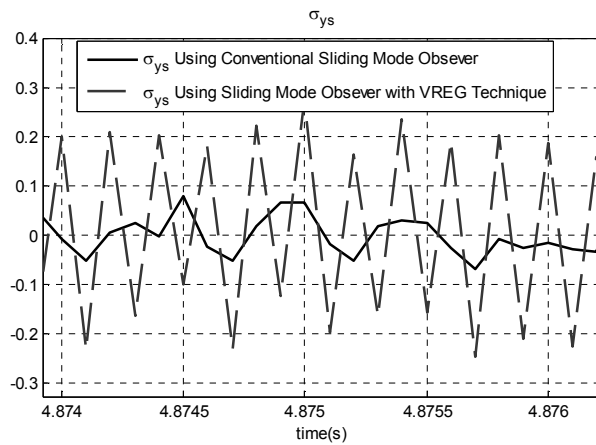


Figure 7. Input signal of the relay σ_{ys} in presence of measurement noise

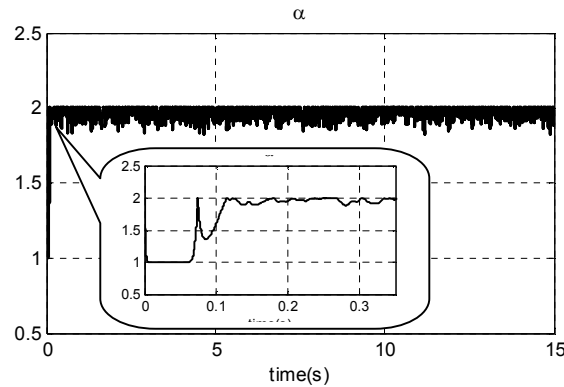


Figure 8. Variation of α using VREG technique

6. CONCLUSION

Designing a relay based sliding-mode observer was introduced in this paper. This observer uses the high gain property of the sliding-mode observer before the switching occurs in order to have fast response and also providing conditions for reaching the sliding surface. Then, in the switching state, signals are decomposed into the slow- and fast-modes. The main contribution of this paper is that it provides a method for analysis of the fast and slow-modes of signals in the switching condition for nonlinear sliding-mode observers. Moreover, it gives the relationship between these modes. In the slow mode, a method is proposed such that the high-gain observer properties are obtained in order to reject this mode. In addition, the fast mode is designed such that 1) the relay equivalent gain provides conditions for good tracking and stability in the slow mode and 2) the frequency of oscillation becomes high enough such that it can be rejected by a simple low pass filter. Furthermore, sensitivity of the observer against the measurement noise was analyzed and it was showed how it can affect the frequency and amplitude of oscillations. At the end of this paper, a variable relay equivalent gain (VREG) technique was proposed to give the observer faster response and less sensitivity to the measurement noise. Simulation results on a bioreactor process showed that the proposed technique provides good tracking and better noise rejection as compared to the fixed equivalent gain technique, which is used in conventional sliding-mode observers.

References

- [1] J. Picó, H. D. Battista, F. Garelli, Smooth sliding-mode observers for specific growth rate and substrate from biomass measurement, *Journal of Process Control*. 19 (2009) 1314–1323.
- [2] S. K. Spurgeon, Sliding mode observers: a survey, *International Journal of Systems Science*. 39 (2008) 751–764.
- [3] K. C. Veluvolu, Y.C. Soh, and W. Cao, Robust observer with sliding mode estimation for nonlinear uncertain systems, *IET Control Theory Appl.* 1 (2007) 1533–1540.
- [4] R. A. López and R. M. Yescas, State estimation for nonlinear systems under model uncertainties: a class of sliding-mode observers, *Journal of Process Control*. 15 (2005) 363–370.
- [5] R. Aguilar, R. Martinez-Guerra, and R. Maya-Yescas, State estimation for partially unknown nonlinear systems: a class of integral high gain observers, *IEE Proc. Control Theory Appl.* 150 (2003) 240–244.

- [6] A. N. Atassi and H. K. Khalil, Separation results for the stabilization of nonlinear systems using different high-gain observer designs, *Systems & Control Letters*. 39 (2000) 183–191.
- [7] J. P. Cunha, R. R. Costa, F. Lizarralde, and L. Hsu, Peaking free variable structure control of uncertain linear systems based on a high-gain observer, *Automatica*. 45 (2009) 1156–1164.
- [8] L. K. Vasiljevic H. and K. Khalil, Error bounds in differentiation of noisy signals by high-gain observers, *Systems & Control Letters*. 57(2008) 856–862.
- [9] J. H. Ahrens and H. K. Khalil, High-gain observers in the presence of measurement noise: A switched-gain approach, *Automatica*. 45 (2009) 936–943.
- [10] D. Q. Mayne, R. W. Grainger, and G. C. Goodwin, Nonlinear filters for linear signal models, *IEE Control Theory and Appl.* 144 (1997) 281–286.
- [11] I. Boiko, Analysis of sliding modes in the frequency domain, *International Journal of Control*. 78 (2005) 969–981.
- [12] Y. Z. Tsytkin, *Relay Control Systems*, Cambridge University Press: Cambridge, U.K., 1984.
- [13] D. P. Atherton, *Nonlinear Control Engineering: Describing Function Analysis and Design*, Van Nostrand Reinhold Co.: London, U.K., 1975.
- [14] I. Boiko and L. Fridman, “Frequency domain input–output analysis of sliding-mode observers,” *IEEE Trans. Autom. Control*. 51 (2006) 1798–1803.
- [15] I. Boiko, Frequency Domain Analysis of Accuracy of Sliding Mode Observers Under Imperfect Knowledge of Model Parameters, *IEEE Trans. Autom. Control*. 54 (2009) 2446–2450.
- [16] I. Boiko, *Discontinuous Control Systems: Frequency-Domain Analysis and Design*, Birkhäuser: Boston, 2008.
- [17] I. Boiko, L. Fridman, A. Pisano, and E. Usai, On the transfer properties of the generalized sub-optimal second-order sliding mode control algorithm, *IEEE Trans. Autom. Control*. 54 (2009) 399–403.
- [18] I. Haskara, U. Ozguner, and V. Utkin, On sliding mode observers via equivalent control approach, *International Journal of Control*. 71(1998) 1051–1067.
- [19] V.I. Utkin. *Sliding modes in control and optimization*, Springer-Verlag: Berlin, 1992.
- [20] K. J. Åström and B. Wittenmark, *Adaptive Control*. Addison-Wesley: Reading, Massachusetts, 1995.
- [21] K. S. Narendra and A. M. Annaswamy, *Stable Adaptive System*, Prentice-Hall: London, 1995.
- [22] J. P. Gauthier, H. Hammouri and S. Othman, A simple observer for nonlinear systems applications to bioreactors, *IEEE Trans. Autom. Control*. 37 (1992) 875–880.
- [23] O. Bernard, G. Sallet and A. Sciandra, Nonlinear observers for a class of biological systems: application to validation of a phytoplanktonic growth model, *IEEE Trans. Autom. Control*. 43 (1998)1056–1065.

- [24] P. Ducommun, A. Kadouri, U. von Stockar, and I. W. Marison, Online determination of animal cell concentration in two industrial highdensity culture processes by dielectric spectroscopy. *Biotechnology and Bioengineering*, 77 (2002), 316–323.
- [25] M. Farza, M. M'Saada, T. Maatouga, and M. Kamounb, Adaptive observers for nonlinearly parameterized class of nonlinear systems, *Automatica*. 45 (2009) 2292–2299.